Improved Generalized Back Projection Algorithm Based on Linearised Sensitivity Function for 3D EIT

Hongbin Wang, Guizhi Xu, Shuai Zhang, Ying Li and Weili Yan
Province-Ministry Joint Key Laboratory of Electromagnetic Field and Electrical Apparatus Reliability,
Hebei University of Technology
No. 8 Guangrongdao, Hongqiao District, Tianjin 300130, P.R. China
Wanghongbin369@163.com

Abstract — 3D Biomedical Electrical Impedance Tomography (EIT) seeks to image the interior conductivity spatial distribution within a 3D object. This approach is improved from generalized back projection algorithm (GBPA) with the purpose of determining projection position of arbitrary part of the 3D object and reconstructing interior conductivity distribution through linearised sensitivity function. To evaluate the proposed method, the improved GBPA is first applied to image reconstruction using a simulated cylinder model. Compared with several algorithms based on back projection method, the images reconstructed by improved GBPA are more accurate in terms of several metrics used in the paper. In addition, the new method reveals good performance to reconstructions from real experimental data.

I. INTRODUCTION

Biomedical Electrical impedance tomography (EIT) attempts to calculate stable and accurate images of interior conductivity distribution of an object from the voltage measurements collected at electrodes surrounding the object when currents are injected. This technology attracts significant research interests for its unique capability of non-invasive detection, real-time monitoring and other advantages in clinical diagnosis [1]-[2].

In this paper we present the method improved from Generalized Back Projection Algorithm (GBPA). Each computation element in the object is put into an imaginary plane which is determined by the position of the couple of injection electrodes and itself. Then we examine this method to quantify several metrics using data calculated from a simulated cylinder model. Additionally the proposed method is applied to reconstructions using data acquired from the 128-channels EIT system [3].

II. IMPROVED GENERALIZED BACK PROJECTION ALGORITHM

In EIT forward problem, Maxwell equations describing the electromagnetic fields inside the object reduce to elliptic equation. Barber states the linearised sensitivity relationship in general condition of conductivity perturbation inside bounded region [4].

$$u_p = -\int_\Omega \sigma_p \nabla \psi_u \cdot \nabla \varphi_u dV \qquad (1)$$

where σ denotes the electric conductivity in the object Ω, ψ and φ are solutions to Maxwell equation and denote potential distribution in the object Ω, subscripts u and p are the uniform and perturbed equivalents respectively

We assume that imaginary elements are substituted for previous subdivision elements. The injection configuration selects one couple of drive-receive electrode mode so as to guarantee monotonicity of the electric field inside the object. Thus there is a unique electric current line via any node inside the object between the couple of injection electrodes so that an imaginary plane can be established to approximate the electric curved surface through the two electrodes and the computation imaginary element. The potential of imaginary element can be calculated through potential function ϕ of Finite Element Method (FEM) and the potential of the subdivision element nodes [5]-[6]. And the boundary voltages of the imaginary plane can be obtained in the same way. The potential of any node v_{im}^i in the imaginary plane corresponds to the value of imaginary boundary voltage fitting curve u_{im}^i.

$$v_{im}^i = f_{u_{im}^i}(x,y) = f_{\phi(u^i)}(x,y) \qquad (2)$$

where u^i denotes the boundary voltage, x and y are the coordinates of electrode axis on the boundary surface, i corresponds to the i^{th} drive pair – receive pair combination.

The imaginary plane is discussed in two conditions for relative position between the couple of injection electrodes and computation object:

(1) The boundary of imaginary plane is bounded to ellipse or circle in the simulated cylinder boundary surface as shown in Fig. 1. (a). In this condition, computation is the same as GBPA forward problem.

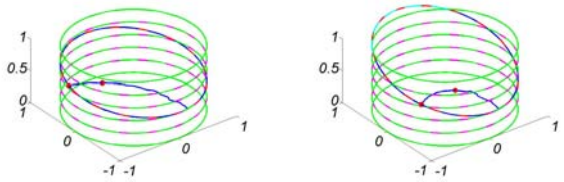

(a) Bounded imaginary plane (b) Incomplete bounded imaginary plane

Fig. 1. Imaginary plane boundary condition

(2) The boundary of imaginary plane is incompletely bounded in the simulate cylinder boundary surface as shown in Fig. 1. (b). In this condition, the imaginary electrode out of the cylinder surface is unavailable to join in computation because its calculated value reflects incorrect potential distribution. For the open structure, the available imaginary boundary voltages can not provide a complete fitting curve.

From the analytical solution to the 3D electrical forward problem for a circular cylinder [7], the value of the

computation object is always in the interval which endpoints are two available adjacent imaginary boundary voltages. Therefore, the projection position can be calculated by the incomplete curve fitting by those consequent available imaginary boundary voltages. Then the projection position of this imaginary element can be presented in the boundary voltage planar distribution.

The conductivity distribution function is normalized as

$$\tilde{\sigma}_n = \tilde{\sigma}_p / \sigma_u \tag{3}$$

From the linearised sensitivity function (1) we have

$$\phi^{-1}\left(f_{v_{im}^i}(x,y)\right) = \frac{-\int_\Omega \tilde{\sigma}_n \nabla\psi_u \cdot \nabla\varphi_u dV}{\int_\Omega \nabla\varphi_u^i \cdot \nabla\psi_u^i dV} \tag{4}$$

Through solving (4) in matrix form, we can reconstruct the normalized conductivity distribution.

III. SIMULATION RESULTS AND COMPARISON

A. Simulation Model and Reconstructed Results

A 3D simulation cylinder model, as shown in Fig. 2, is established to assess the performance of improved GBPA. Three targets are chosen to represent organs in human body, and the conductivities of them are assumed different from those of other tissues.

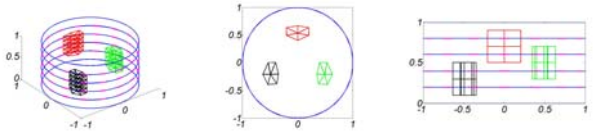

(a) Lateral view (b) Top view (c) Front view

Fig. 2. Three views of 3D cylinder model with three targets

We choose successive adjacent drive-receive electrode configuration on every layer of electrode array from section 1 (bottom) to 4 (top). The reconstructed images are shown in Fig. 3.

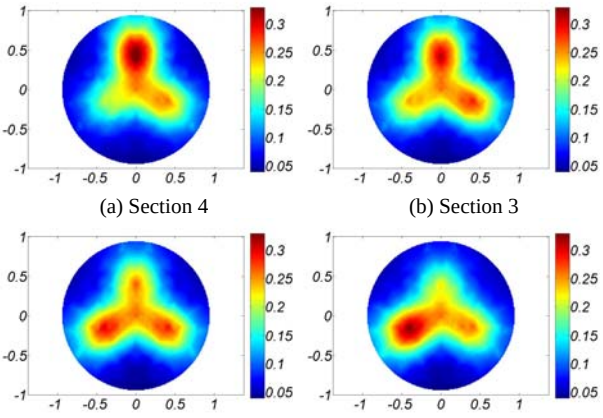

(a) Section 4 (b) Section 3

(c) Section 2 (d) Section 1

Fig. 3. Reconstructed results of simulation model

B. Comparison by Evaluation parameters

To quantitatively interpret the reconstruction results, we use four metrics from [1]: Position error (PE), Resolution (RES), Shape deformation (SD), Information Entropy (IE). In order to compare conventional Back Projection Algorithm (BPA), Node Back Projection Algorithm (NBPA) [8] and GBPA with improved GBPA, The four parameters are computed and showed in TABEL I.

TABLE I
COMPARISON OF BPA NPBA GBPA AND IMPROVED GBPA

	PE	RES	SD	IE
BPA	0.35006	0.48304	0.32954	40.302
NBPA	0.34546	0.42007	0.31925	40.467
GBPA	0.33573	0.41751	0.31573	40.493
Improved GBPA	0.32847	0.40768	0.30933	40.536

The results indicate that reconstructed targets by improved GBPA have lower position error and better shape deformation in the comparison of BPA, NBPA and GBPA. In terms of resolution, lowest value of improved GBPA demonstrates serving primarily to distinguish nearby targets. Also, the reconstructed images of improved GBPA contain more image information of conductivity distribution.

IV. CONCLUSION

Additionally we take the proposed algorithm to reconstruct real images inside experimental phantom using data collected from the 128-channel EIT system [3].

The reconstructed results both of simulation experiment and real experiment show good performance of improved GBPA, and indicate that the proposed method can provide more help to diagnosis.

ACKNOWLEDGMENT

This work was supported in part by the National Natural Science Foundation of China under Grant No. 50937005 and No. 51077040.

V. REFERENCES

[1] Adler A., Arnold J. H., Bayford R., et al, “GREIT: a unified approach to 2D linear EIT reconstruction of lung images”, *Physiol. Meas.*, Vol. 30, pp. S35-S55, 2009.

[2] Fabrizio Ferraioli, Alessandro Formisano, Raffaele Martone, “Effective Exploitation of Prior Information in Electrical Impedance Tomography for Thermal Monitoring of Hyperthermia Treatments”, *IEEE Transactions on Magnetics*, Vol. 45, No. 3, pp. 1554-1557, 2009.

[3] Guizhi Xu, Renping Wang, Shuai Zhang, et al, “A 128-Electrode Three Dimensional Electrical Impedance Tomography System”, *IEEE EMBC 2007, 29th Annual International Conference*, France, pp. 4386-4389, 2007.

[4] Barber D. C., “Image Reconstruction in Applied Potential Tomography – Electrical Impedance Tomography”, *Internal Report, Department of Medical Physics and Clinical Engineering, University of Sheffield*, 1990.

[5] Guizhi Xu, Huanli Wu, Shuo Yang, et al, “3-D Electrical Impedance Tomography Forward Problem with Finite Element Method”, *IEEE Transactions on Magnetics*, Vol. 41, No. 5, pp. 1832-1935, 2005.

[6] Guoya Dong, J. Zou, Richard Bayford, et al, “The Comparison between FVM and FEM for EIT Forward Problem”, *IEEE Transactions on Magnetics*, Vol. 41, No. 5, pp. 1468-1471, 2005.

[7] Kleinermann F., Avis N. J., Alhargan F. A., “analytical solution to the three-dimensional electrical forward problem for a circular cylinder”, *Inverse Problems*, Vol. 16, pp. 461-468, 2000.

[8] Jianjun Zhang, Weili Yan, Guizhi Xu, et al, “A New Algorithm to Reconstruct EIT Images: Node-Back-Projection Algorithm”, *IEEE EMBC 2007, 29th Annual International Conference*, France, pp. 4390-4393, 2007.